European Journal of Pharmaceutics and Biopharmaceutics 78 (2011) 67–74

Contents lists available at ScienceDirect

European Journal of Pharmaceutics and Biopharmaceutics

journal homepage: www.elsevier.com/locate/ejpb

Research paper

Plasma deposited stability enhancement coating for amorphous ketoprofen

Stephanie Bosselmann [a,*], Donald E. Owens III [b], Rachel L. Kennedy [b], Matthew J. Herpin [b], Robert O. Williams III [a]

[a] Division of Pharmaceutics, The University of Texas at Austin, Austin, United States
[b] AeonClad Biomedical LLC, Austin, United States

ARTICLE INFO

Article history:
Received 7 July 2010
Accepted in revised form 8 December 2010
Available online 15 December 2010

Keywords:
Plasma-enhanced chemical vapor deposition
Amorphous drug
Recrystallization
Physical stability
Fluorocarbons

ABSTRACT

A hydrophobic fluorocarbon coating deposited onto amorphous ketoprofen via pulsed plasma-enhanced chemical vapor deposition (PPECVD) significantly prolonged the onset of recrystallization compared to uncoated drug. Rapid freezing (RF) employed to produce amorphous ketoprofen was followed by PPECVD of perfluorohexane. The effect of coating thickness on the recrystallization and dissolution behavior of ketoprofen was investigated. Samples were stored in open containers at 40 °C and 75% relative humidity, and the onset of recrystallization was monitored by DSC. An increase in coating thickness provided enhanced stability against recrystallization for up to 6 months at accelerated storage conditions (longest time of observation) when compared to three days for uncoated ketoprofen. Results from XPS analysis demonstrated that an increase in coating thickness was associated with improved surface coverage thus enabling superior protection. Dissolution testing showed that at least 80% of ketoprofen was released in buffer pH 6.8 from all coated samples. Overall, an increase in coating thickness resulted in a more complete drug release due to decreased adhesion of the coating to the substrate.

1. Introduction

Amorphous solids are generally characterized by a short range order in their atomic arrangement while the long range order, found in crystalline compounds, is absent. The less ordered and more entropic amorphous state has a correspondingly higher free energy when compared to the crystalline state and this directly translates into an increased apparent solubility and dissolution [1,2]. Based on this, the formulation of drugs in the amorphous state has become an attractive way to overcome bioavailability problems associated with poorly water-soluble drugs. Despite the advantages that amorphous compounds can offer in drug delivery, there is significant concern regarding their stability. Due to their higher energetic state, amorphous compounds have the tendency to convert to the more stable, less energetic crystalline form. As a result, changes in the release characteristics and accordingly in the bioavailability may occur during long-term storage of amorphous formulations [3,4]. Storage temperature and water content of the amorphous composition have been identified as key factors influencing the rate of crystallization. As the storage temperature nears or exceeds the glass transition temperature (T_g) of the amorphous solid, the molecular mobility and consequently the rate of crystallization are significantly increased [5]. In addition, the presence of water (e.g. in the case of the drug being exposed to humidity) can accelerate crystallization of a metastable amorphous system. Unlike crystalline solids, which adsorb water simply on the surface, amorphous materials have the ability to absorb significant amounts of moisture into their internal structure [6]. The absorbed water leads to an increase in free volume and molecular mobility of the amorphous phase thereby promoting crystallization.

The most common approach of stabilizing amorphous drugs is the addition of high T_g polymers such as hydroxypropylmethylcellulose or polyvinylpyrrolidone [7–9]. Their stabilizing effect has been primarily attributed to an increase in the T_g, the disruption of drug–drug interactions and the formation of drug–polymer interactions [10–12]. However, the types of polymers used are generally hydrophilic and therefore increase the hygroscopicity of the system [13].

Barrier coatings have been suggested as another potential way to increase stability of amorphous compounds by primarily functioning as a physical barrier that reduces surface mobility. Wu et al. have reported that an ultrathin polyelectrolytes coating deposited by an electrostatic layer-by-layer assembly of cationic poly(dimethyldiallyl ammonium chloride) and anionic sodium poly(styrenesulfonate) in aqueous solution successfully inhibited surface crystallization of amorphous indomethacin when stored at a temperature slightly below its T_g [14]. Additionally, Zhu and coworkers described the inhibitory effect of a 10 nm gold coating

* Corresponding author. The University of Texas at Austin, College of Pharmacy, 1 University Station, Mail Stop A1920, Austin, TX 78712, United States. Tel.: +1 512 471 8469; fax: +1 512 471 7474.
E-mail address: sbosselmann@mail.utexas.edu (S. Bosselmann).

0939-6411/$ - see front matter © 2010 Elsevier B.V. All rights reserved.
doi:10.1016/j.ejpb.2010.12.011

on the surface crystallization of nifedipine when stored at elevated temperature [15].

Considering the plasticizing effect of water, the aim of the present study was to provide a physical and at the same time moisture-resistant barrier coating capable of inhibiting crystallization of an amorphous drug/polymer system. Plasma polymerization, also known as plasma-enhanced chemical vapor deposition (PECVD), a dry coating method, was chosen to deposit thin hydrophobic polymer films on the surface of amorphous ketoprofen (KET)/Methocel™ E5 aggregate particles. Though conventional liquid-based coating methods have been well established and widely adopted by the pharmaceutical industry, they can be problematical when utilized for the coating of amorphous compositions: elevated temperatures during drying and the presence of water carry the risk of inducing crystallization during the coating process. Further disadvantages of wet coating methods include long processing times, the problem of residual solvents and the non-applicability for the coating of nanoparticles due to agglomerate formation [16–18]. By eliminating the use of water or organic solvents, dry coating methods like PECVD are able to overcome several of the shortcomings associated with wet coating technologies. Specifically, PECVD allows deposition of thin films on a wide variety of substrates, including sub-micron particles, in a room temperature, one-step process [19]. It involves the fragmentation of gaseous monomers into activated species, mainly free radicals and ions, which then recombine and condense on the surface of the substrate as a solid polymer film (i.e. *in situ* polymerization). The energy needed for monomer activation is provided by the plasma, which can be induced by a variety of sources including radiofrequency and microwave radiation [20]. PECVD-polymers can be considered an entirely new class of materials enabling custom-tailoring of surface properties including chemical inertness, enhanced reactivity, hardness and wettability, only to mention a few [21]. Therefore, it is not surprising that PECVD has become an attractive tool in the biomedical and pharmaceutical fields and has been used for a wide variety of applications from increasing biocompatibility and cell adhesion to controlling drug release [22–25].

The objective of the present study was to investigate the ability of hydrophobic plasma-polymerized films to prevent crystallization of amorphous KET. It was hypothesized that the films would stabilize the amorphous system by reducing surface mobility and preventing water vapor absorption. Rapid freezing, a cryogenic particle engineering technology, was employed to produce amorphous aggregates of KET and Methocel™ E5 (RF-KET) [26]. The deposition of films onto RF-KET was conducted utilizing a pulsed PECVD method. Pulsed PECVD methods have been previously demonstrated to provide excellent film chemistry and thickness control [27]. Films were plasma polymerized from perfluorohexane (C_6F_{14}), a monomer known to form highly hydrophobic films therefore allowing very limited water vapor penetration [28]. In addition, C_6F_{14} is practically non-toxic when taken orally suggesting that it is an adequate excipient for the formulation of oral dosage forms [29].

Properties of uncoated and plasma-coated RF-KET were investigated employing a wide variety of techniques. Furthermore, the effect of coating thickness on the process of crystallization and dissolution behavior was evaluated.

2. Materials and methods

2.1. Materials

Ketoprofen, USP was purchased from Hawkins, Inc. (Minneapolis, MN). Methocel™ E5 Premium LV (hydroxypropylmethylcellulose) was obtained from The Dow Chemical Company (Midland, MI) and 1,4-dioxane and HPLC-grade acetonitrile were purchased from Fisher Scientific (Fair Lawn, NJ). Perfluorohexane (C_6F_{14}) was obtained from VWR (West Chester, PA) and consisted primarily of the n-isomer. Additionally, perfluorohexane monomers were out-gassed via three consecutive freeze thaw cycles under vacuum prior to every plasma deposition application to ensure purity and the removal of any dissolved oxygen. All other chemicals utilized in this study were at least of ACS grade.

2.2. Preparation of RF-KET

RF-KET was prepared by dissolving KET and Methocel™ E5 at a 1:1 ratio in a 1,4-dioxane/purified water (65/35, v/v) co-solvent system yielding a 1% (w/v) solid concentration. The feed solution was then fed as discrete droplets onto a chilled rotating drum maintained at approximately −60 °C. The frozen material was collected and dried using a bench top tray lyophilizer (The VirTis Company, Inc., Gardiner, NY).

2.3. Pulsed plasma-enhanced chemical vapor deposition (PPECVD)

Thin films were deposited onto RF-KET (as obtained under Section 2.2) using a cylindrical, 360° rotatable plasma reactor with a volume of approximately 900 cm^3. The C_6F_{14} gaseous monomer was introduced into the reactor and energized into plasma by an electrical discharge from a radiofrequency generator. Specifically, a 13.56 MHz PPECVD process with a peak power of 150 W and a duty cycle of 10 ms on and 40 ms off at a pressure of 160 mTorr and a monomer flow rate of 100 sccm was utilized to deposit polymerized films onto the surface of RF-KET. The deposition time was varied (Table 1) to obtain three samples with different coating thicknesses (RF-KET-CF_x low, RF-KET-CF_x medium, RF-KET-CF_x high).

2.4. Drug potency

The KET potency (w/w%) of uncoated and coated powders was determined by dissolving a known amount of dry powder in 100 mL of acetonitrile: phosphate buffer pH 4 (55:45, v/v). Aliquots were then analyzed for KET content using a Shimadzu VP-AT series LC10 HPLC system with a photodiode array detector (Model 996) extracting at a wavelength of 256 nm. The mobile phase consisted of acetonitrile: phosphate buffer pH 4 (55:45, v/v). KET was eluted from an Inertsil 5 μm ODS-2 column (4.6 mm i.d. ×150 mm; GL Sciences Inc.) at approximately 3.9 min.

2.5. Differential scanning calorimetry (DSC)

DSC was conducted using modulated temperature DSC (MTDSC), Model 2920 (TA Instruments, New Castle, DE). Samples were weighed to 5–10 mg in aluminum crimped pans and heated at a ramp rate of 10 °C/min from 5 to 200 °C using a modulation temperature amplitude of 1 °C and a modulation period of 60 s. Dry nitrogen gas was used as the purge gas through the DSC cell

Table 1
Coating times and KET potency (% w/w) of RF-KET (RF processed ketoprofen:Methocel™ E5 = 1:1), RF-KET-CF_x low (RF-KET coated with C_6F_{14} – low thickness), RF-KET-CF_x medium (RF-KET coated with C_6F_{14} – medium thickness) and RF-KET-CF_x high (RF-KET coated with C_6F_{14} – high thickness).

Sample	Coating time (min)	KET potency (%w/w)
RF-KET	N/A	49.84 ± 0.45
RF-KET-CF_x low	20	49.61 ± 0.52
RF-KET-CF_x medium	45	49.42 ± 0.20
RF-KET-CF_x high	480	46.81 ± 0.39

at a flow rate of 40 mL/min. All data were analyzed using TA Universal Analysis 2000 software (TA Instruments, New Castle, DE) and are presented in terms of reverse heat flow.

2.6. Dissolution testing

Dissolution testing was performed using the paddle apparatus at 50 rpm (Vankel 7000 Dissolution Tester, Vankel Technology Group, Cary, NC). Specifically, freshly prepared formulations were tested in McIlvaine's buffer pH 6.8. The medium was held at 37.0 ± 0.2 °C throughout the test procedure. Each dissolution vessel contained approximately 5 mg KET equivalent. Aliquots of dissolution media were sampled and filtered through 0.2-μm GHP filters. Filtered aliquots were then diluted in a 1:1 ratio with acetonitrile and analyzed for drug content using a Shimadzu VP-AT series LC10 HPLC system with a photodiode array detector (Model 996) extracting at a wavelength of 256 nm. The mobile phase consisted of acetonitrile: phosphate buffer pH 4 (55:45, v/v). KET was eluted from an Inertsil 5 μm ODS-2 column (4.6 mm i.d. ×150 mm; GL Sciences Inc.) at approximately 3.9 min. The area under the dissolution curve for all coated samples was compared for statistical significance by using one-way ANOVA at a level of $p < 0.05$ (JMP®7 Software).

2.7. Scanning electron microscopy (SEM)

Samples were mounted onto an aluminum stage and sputter-coated with silver for 30 s. Particle morphology was evaluated employing a LEO-1530 SEM operated at an accelerating voltage of 10 kV.

2.8. X-ray photoelectron spectroscopy (XPS)

XPS was used to analyze the elemental surface composition of RF-KET and RF-KET-CF_x low, medium and high. Additionally, a double polished silicon wafer was coated with the same monomer (C_6F_{14}) and plasma conditions used for coating the RF-KET powders to act as a control and reference material for XPS testing. Measurements were performed on an AXIS HS photoelectron spectrometer (Kratos Analytical, UK) using a monochromatic Al Kα X-ray source. A take-off angle of the photoelectrons perpendicular to the sample holder was used throughout. Peaks were fitted using a nonlinear least-square curve fitting program (XPS®PEAK 4.1 software) with mixed Gauss–Lorentz product function and Shirley background. Areas under selected photoelectron peaks in the spectrum were used to estimate atomic concentrations in percent.

2.9. Time-of-flight secondary ion mass spectrometry (ToF-SIMS)

ToF-SIMS was used to probe the molecular composition in the uppermost 1–3 monolayers of the sample. Measurements were performed using a TOF.SIMS (ION-TOF, Münster, Germany), equipped with a Bi cluster ion source. Mass resolved secondary ion images from a field of view of 500 × 500 μm^2 were obtained using Bi_3^+ primary ions at 25 keV energy (DC current 500 pA; target current 0.06 pA). The lateral resolution was 300 nm. The images were taken at nominal mass resolution in positive secondary ion polarity. For representation of aromatic and F containing organic species, the image intensities of characteristic masses (aromatic species: $C_6H_5^+$, $C_6H_7^+$, $C_7H_7^+$, $C_8H_9^+$; F containing species: C^+, F^+, CF^+, $C_7F_9^+$) were added up. Before doing so it was ensured that the images show the same lateral distribution. As the sample shows a distinct topography, the images were normalized to the total ion image in order to reduce the influence of topography to the image appearance.

2.10. Contact angle

Dry powder (50 mg) was compressed with a 1500 kg compression force using a Carver Laboratory Press (Model M, Fred S. Carver Inc., WI) equipped with 6 mm diameter flat-faced punches. A 5 μL drop of McIlvaine's buffer pH 6.8 was placed on the surface of the tablet, and the contact angle was determined by measuring the tangent to the curve of the droplet on the surface of the compact using a goniometer (Model No. 100-00-115, Rame-Hart Inc., Mountain Lakes, NJ).

2.11. Stability testing

To evaluate stability, RF-KET and plasma-coated samples (RF-KET-CF_x low, medium and high) were stored in open containers at elevated temperature and humidity. Specifically, samples were stored in a sealed humidity chamber containing a saturated sodium chloride solution to create a 75% relative humidity environment and then stored in an oven maintained at 40 °C. The process of crystallization was monitored using DSC and SEM.

3. Results and discussion

3.1. Physicochemical properties of uncoated and plasma-coated RF-KET

SEM pictures of bulk crystalline KET (Fig. 1a) displayed dense rod-shaped crystals ranging in size from 5 to 10 μm. On the contrary, pictures of RF-KET (Fig. 1b and c) revealed an interconnected porous network of KET/Methocel™ E5 strands. The same structure was observed for all plasma-coated samples (pictures not shown), indicating the PPECVD process did not alter the substrate morphology. In fact, one of the most important advantages of plasma polymerization lies in its ability to drastically change surface properties without changing the bulk properties of the material [30]. In this study, the hydrophilic surface of RF-KET was extremely hydrophobized by polymerization of C_6F_{14} as indicated by an increase in the contact angle from 51° (RF-KET) to approximately 100° for all coated samples (Table 2). Perfluorocarbons are characterized by an exceptional inertness, which relates to the strength of the carbon–fluorine bond, the strongest single bond found in organic chemistry [28]. The inert surface of fluorocarbons is responsible for their extreme hydrophobicity since it does not allow for sufficient hydrogen bonding with approaching water molecules. Accordingly, fluorocarbons are very effective as barriers to moisture permeation.

The KET content (w/w%) of uncoated RF-KET as well as RF-KET-CF_x low and medium was determined to be 49.84%, 49.61% and 49.42%, respectively (Table 1). The minimal difference in drug potency between uncoated RF-KET and the samples with low and medium thickness indicates that very thin coatings in the nanometer range were deposited. A drug loading of 46.81% for RF-KET-CF_x high demonstrates a much thicker fluorocarbon coating was deposited, which is in accordance with the significantly longer coating time applied for this sample. Previous studies utilizing pulsed plasma polymerization have demonstrated a linear relationship between deposition time and film thickness [27,31].

Even though plasma polymerization represents an attractive way of tailoring surface characteristics of a wide variety of substrates, considerable degradation of the substrate may occur during the process due to vacuum ultraviolet and ultraviolet radiation as well as substrate bombardment through high-energy species [32]. The use of a pulsed plasma mode, as utilized in this study, significantly reduces the risk of substrate degradation when compared to the continuous wave mode. In particular, the number of reactive species and the photon flux are reduced in the pulsed

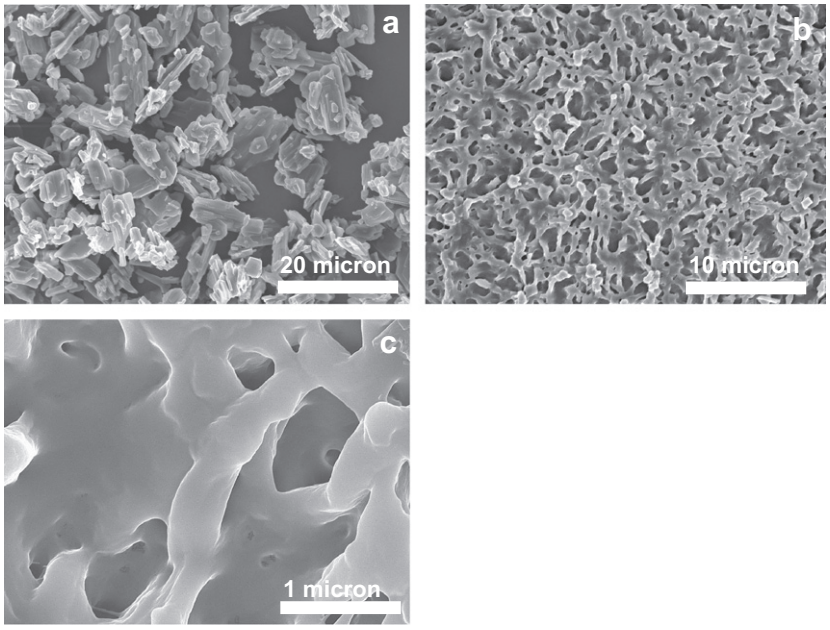

Fig. 1. SEM images of (a) bulk crystalline ketoprofen, (b) RF-KET (RF processed ketoprofen:Methocel™ E5 = 1:1), (c) RF-KET at a higher magnification.

Table 2
Percentage of each component, F/C ratio and contact angle of RF-KET coated with C_6F_{14} for different time intervals.

	RF-KET-CF_x low	RF-KET-CF_x medium	RF-KET-CF_x high
CF_3 (%)	23.01	26.75	29.04
CF_2 (%)	24.50	31.13	28.31
CF—CF_x (%)	11.36	14.53	11.89
CF (%)	8.68	9.62	10.63
C—CF_x (%)	19.80	14.83	14.60
C—C (%)	12.65	3.14	2.31
F/C ratio	1.45	1.57	1.63
Contact angle	96.80	100.25	102.00

plasma approach as many of the short-lived excited species decay during the off-portion of the duty cycle. Accordingly, no KET degradation peaks were observed in HPLC chromatograms of all coated samples.

3.2. Thermal analysis of uncoated and plasma-coated RF-KET

Amorphous KET is highly unstable and recrystallizes spontaneously at room conditions [33]. A concentration of 50% (w/w) Methocel™ E5 was found to be sufficient to stabilize KET. Concentrations of more than 50% (w/w) KET resulted in formulations with T_g's close to or even below room temperature. Consequently, those products were softened when collected from the lyophilizer and therefore found unsuitable for this study.

DSC thermograms of quench-cooled KET, RF-KET, the corresponding physical mixture of KET and Methocel™ E5 (1:1) and plasma-coated powders are shown in Fig. 2. The T_g of amorphous KET and Methocel™ E5 were observed at −5.22 °C and 144.33 °C, respectively. The melting endotherm for crystalline KET at approximately 96 °C, which can be seen with the physical mixtures of KET and Methocel™ E5, is absent for RF-KET indicating that the drug was rendered entirely amorphous by RF processing. The theoretical T_g of RF-KET was predicted utilizing the Gordon–Taylor Eq. (1) for binary mixtures [34]:

$$T_g = \frac{w_1 T_{g1} + K w_2 T_{g2}}{w_1 + K w_2} \quad (1)$$

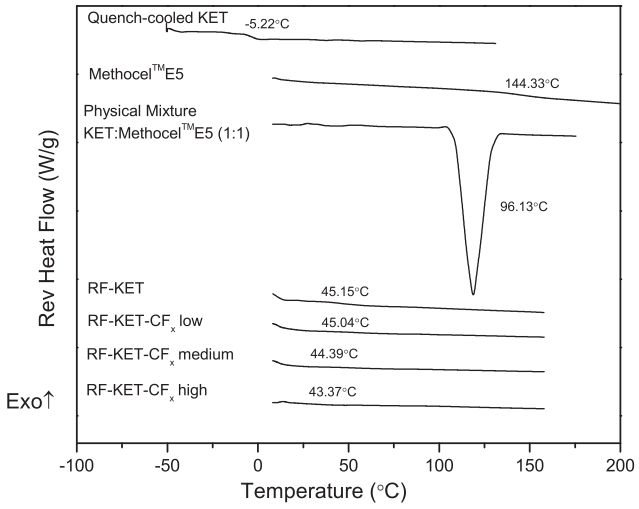

Fig. 2. DSC thermograms of samples stored in a desiccator under vacuum at room temperature.

where w_1 and w_2 are the mass fractions of KET and Methocel™ E5, and T_{g1} and T_{g2} are the respective glass transition temperatures. The constant K can be calculated according to the Simha–Boyer rule presented in Eq. (2) [35]:

$$K = \frac{\rho_1 T_{g1}}{\rho_2 T_{g2}} \quad (2)$$

where ρ_1 and ρ_2 are the densities of the two components as determined by helium pycnometry.

According to the Gordon-Taylor equation, the T_g of RF-KET was determined to be 53.52 °C, while the actual T_g was observed at 45.15 °C. Deviations from expected T_g values are generally ascribed to differences in the strength of intermolecular interactions between the single components and those of the blend. Specifically, a negative deviation from the theoretical value, as for RF-KET, indicates less strong interaction between the components of the mixture. This can for example be the case if one component has

the tendency to self-associate due to the existence of specific functional groups, like carboxylic or amide groups [36]. Since KET has a carboxylic group, the deviation between the actual and predicted T_g value of RF-KET is possibly due to stronger drug–drug interactions compared to drug–polymer interactions.

In DSC thermograms for all coated RF-KET samples, the KET melting endotherm is also missing demonstrating the amorphous character of KET was preserved during PPECVD. The PPECVD is a very gentle dry coating process allowing for film growth at room temperature. Based on the process conditions, it is particularly suitable for the coating of amorphous material.

3.3. XPS/ToF-SIMS

In contrast to conventional linear polymers, plasma polymers are characterized by a more complex branched structure. During plasma polymerization, several reactive species including electrons, ions and reactive neutrals are produced, all of which influence the growing polymer film resulting in a cross-linked polymer network. To give some indication of the chemical structure and the degree of cross-linking of CF_x-coatings deposited on RF-KET, XPS was conducted (Fig. 3). A thin polymer film, plasma polymerized from C_6F_{14} onto a double polished silicon wafer (CF_x wafer), was used as a reference and the following peak assignments were made: CF_3 (293 eV), CF_2 (291 eV), CF—CF_x (288.8 eV), CF (287.7 eV) and C—CF_x (286.7 eV). All peaks present in the CF_x wafer spectrum were also found in the spectra of RF-KET-CF_x low, medium and high. The films deposited are rich in CF_2 and CF_3 groups (Table 2), demonstrating a very linear polymer structure was obtained, which can be attributed to the pulsed PECVD mode. Several studies have demonstrated that the pulsed PECVD mode, in contrast to the continuous wave mode, provides polymer films exhibiting highly ordered linear structures [37–39]. The higher linearity can be mainly attributed to a lower substrate temperature, reduced ion-bombardment of the growing polymer film and less intense UV radiation [37].

Furthermore, the F/C ratio, a measure for the extent of surface fluorination, was calculated from the curve-fitted C1*s* spectra using Eq. (3) [40]:

$$\frac{F}{C} = \frac{(3 \times \%CF_3) + (2 \times \%CF_2) + (\%CF)}{100} \quad (3)$$

The films deposited onto RF-KET have F/C ratios of around 1.5–1.6 compared to an F/C ratio of 2.3 for the starting monomer (Table 2). With increasing deposition time, more fluorine-rich and therefore hydrophobic films were obtained as indicated by an increase in the F/C ratio. This observation is in accordance with an increase in the contact angle attributed to increasing deposition time. The same trend has been observed by Mukhopadhyay et al. who reported the contact angle of a porous substrate treated with a fluorocarbon coating increased with increasing coating time until a maximum value was reached [41].

The analysis of the C1*s* core level spectra for uncoated RF-KET yielded four peaks: C—C (284.4 eV), C—O (286.4 eV), C=O/O—C—O (288.2 eV) and O—C=O (290 eV). Core level spectra of plasma-coated samples are expected to show (1) peaks corresponding to the coating and depending on the thickness and uniformity of the coating (2) peaks corresponding to uncoated RF-KET core level components. As an indicator for the presence of RF-KET, the C—C peak was chosen since it displays the highest intensity and at a binding energy that does not overlap with core level components of the coating. Since the escape depth of photoelectrons Al K alpha excitation is restricted to a few nanometers the C—C peak is expected to become increasingly smaller on samples with higher coating thickness. A corresponding trend was in fact observed in the XPS spectra shown in Fig. 3c–e. The circumstance that the C—C peak is still visible even for the sample with the highest coating thickness can be ascribed to the fact that there is always a small

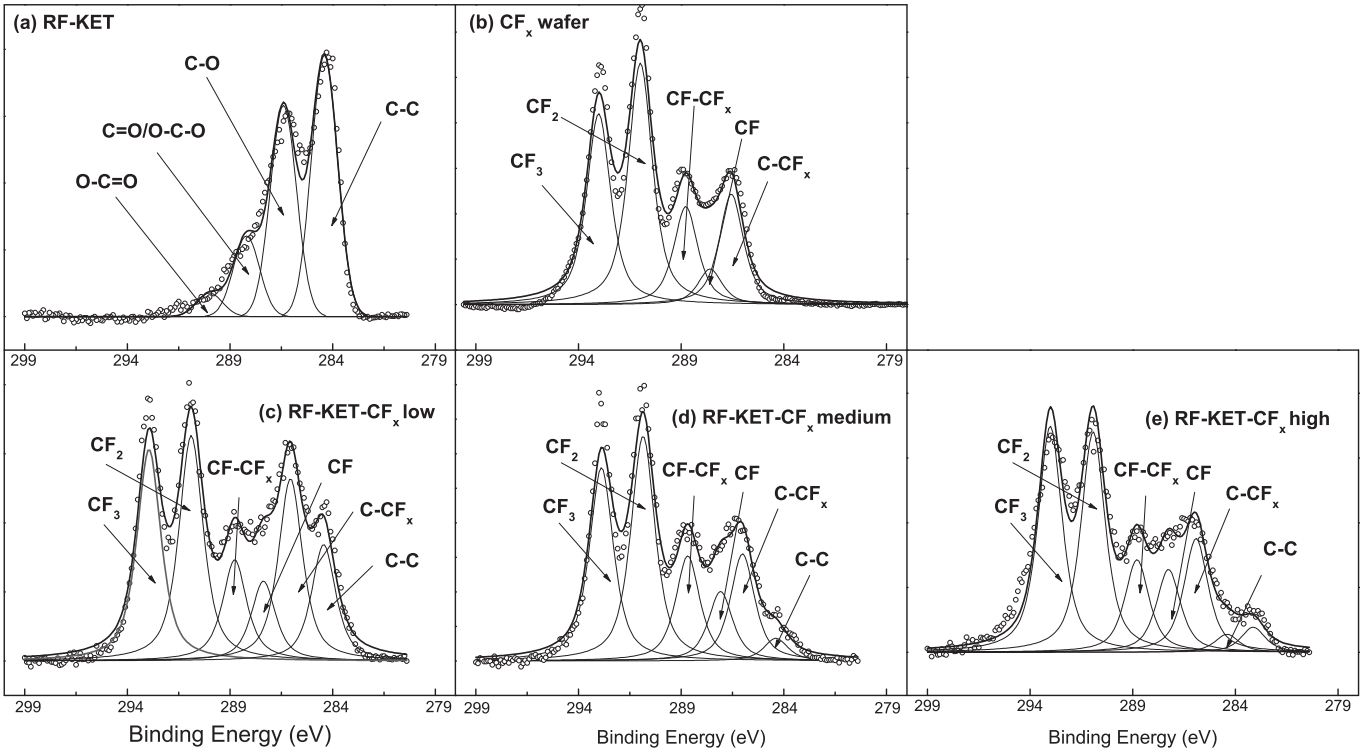

Fig. 3. High resolution C1*s* XPS spectra of (a) RF-KET (RF processed ketoprofen:Methocel™ E5 = 1:1), (b) CF_x wafer (double polished silicon wafer coated with C_6F_{14}), (c) RF-KET-CF_x low (RF-KET coated with C_6F_{14} – low thickness), (d) RF-KET-CF_x medium (RF-KET coated with C_6F_{14} – medium thickness), and (e) RF-KET-CF_x high (RF-KET coated with C_6F_{14} – high thickness).

tail of the photoelectron yield originating from deeper layers (i.e. the RF-KET matrix) and to the non-flat substrate surface formed by the compression of coated aggregate particles.

In addition to XPS, ToF-SIMS scans of RF-KET-CF_x low (Fig. 4) were performed and while a uniform and nearly complete coating was observed, small areas of very thin or missing coating were present. This observation is consistent with the results of stability analysis, showing partial crystallization on samples with thin coating layers, most likely seeded by areas with incomplete coating.

3.4. Dissolution testing

Dissolution profiles of RF-KET, RF-KET-CF_x low, RF-KET-CF_x medium and RF-KET-CF_x high are presented in Fig. 5. As expected, uncoated RF-KET showed the most rapid release with 100% of the drug in solution within 10 min. Given the hydrophobic nature of the CF_x-coating, drug release from the RF-matrix was expected to be greatly reduced. However, this is not reflected in the dissolution profiles: at least 80% of drug was released from all coated samples, after 45 min. RF-KET-CF_x high initially showed the slowest release rate. However, after 30 min the amount of drug released from RF-KET-CF_x low and medium did not significantly increase any further, while drug release from RF-KET-CF_x high continued with 90% of KET in solution after 180 min, compared to 81% and 83% for RF-KET-CF_x low and medium, respectively. The CF_x films deposited on the RF-KET substrate exhibit an extreme hydrophobic character with a water contact angle of approximately 100 (Table 2). The hydrophobicity of the coating does not allow for sufficient wetting meaning the contact area between coated RF-KET and the dissolution media is very limited. Nevertheless, limited water penetration into hydrophobic films through coating defects or pores in the subnanometer to low nanometer range produced by surface roughness has been reported [42–44]. It is assumed water penetration leads to rupture of the coating once a certain stress threshold is exceeded. This assumption is consistent with the observation of 'empty' coating shells present in the dissolution vessel at the end of testing. Naturally, a thinner coating will rupture faster leading to a faster drug release, which can be seen during the first 30 min of dissolution testing. However, after 180 min of testing RF-KET-CF_x high reached the highest concentration and RF-KET-CF_x low the lowest concentration of KET, suggesting that an increase in coating thickness is associated with an increase in drug release. This can be explained with the fact that the thickness of fluorocarbon coatings directly influences their adhesion properties. Lewis and coworkers have investigated the adhesion properties of fluorocarbon coatings of different thicknesses deposited on stainless steel by plasma polymerization [45]. The adhesion

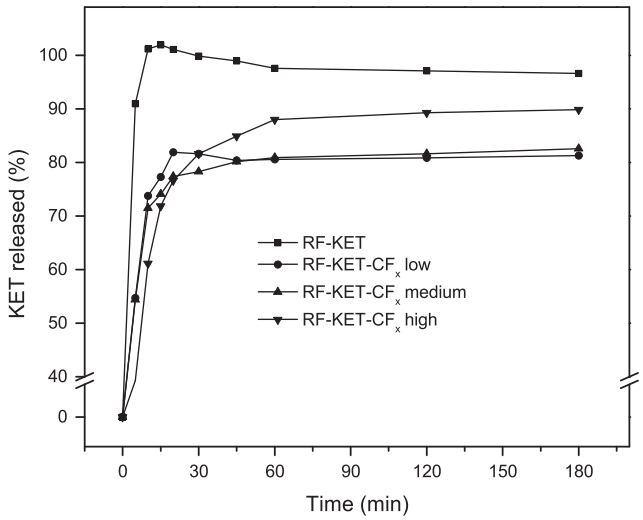

Fig. 5. Dissolution profiles of RF-KET (RF processed ketoprofen:Methocel™ E5 = 1:1), RF-KET-CF_x low (RF-KET coated with C_6F_{14} – low thickness), RF-KET-CF_x medium (RF-KET coated with C_6F_{14} – medium thickness) and RF-KET-CF_x high (RF-KET coated with C_6F_{14} – high thickness) in McIlvaine's buffer pH 6.8 under sink conditions using the paddle apparatus at 50 rpm and 37 °C (error bars omitted for clarity).

properties of a 36 nm thick coating were found to be superior over coatings having a thickness of 100 nm and higher. This suggests adhesion of the CF_x-coating is much stronger for RF-KET-CF_x low and medium, and it is likely that not all of the coating was removed from the RF-KET matrix during dissolution testing leading to an incomplete drug release. On the other hand, a less firm attachment of the polymer film to the RF-KET matrix in the case of RF-KET-CF_x high allows for almost complete coating removal and drug release within the three hour time frame of the dissolution study. Overall, it has to be noted that statistical analysis showed that the areas under the dissolution curves for all coated samples are not significantly different from each other.

3.5. Stability testing at 40 °C and 75% RH

Results from DSC analysis of uncoated RF-KET as well as plasma-coated samples subjected to 40 °C and 75% RH are shown in Fig. 6. After three days of storage, DSC thermograms of uncoated RF-KET revealed the presence of a melting endotherm (T_m: 92.13 °C) attributed to recrystallization of KET. The results from DSC were confirmed by SEM pictures (Fig. 7a), which

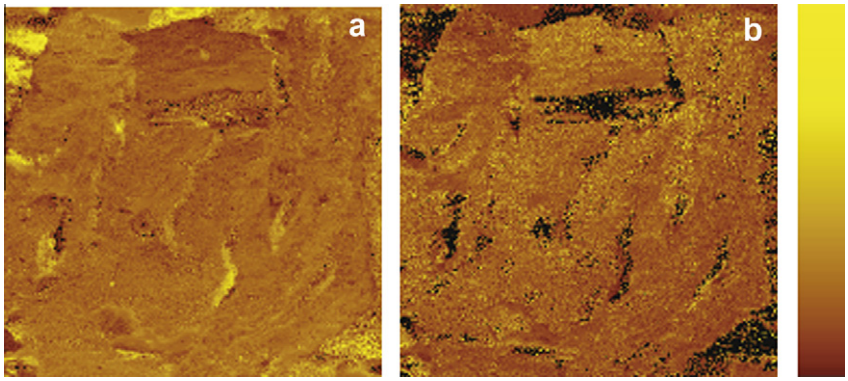

Fig. 4. ToF-SIMS images of RF-KET-CF_x low: (a) CF_x, (b) aromatic hydrocarbons (corresponding to KET); scale on the right is normalized to the brightest pixel in the image: dark – low intensity, bright – high intensity. (For interpretation of the references to colour in this figure legend, the reader is referred to the web version of this article.)

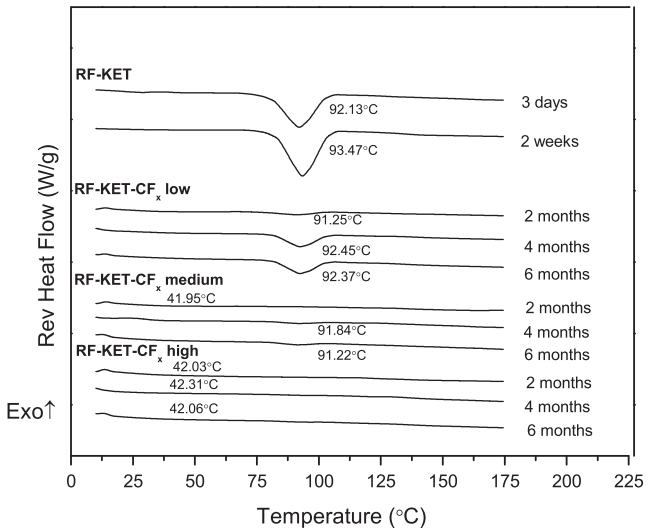

Fig. 6. DSC thermograms of samples stored in open containers at 40 °C and 75% RH.

displayed large KET crystals with none of the original RF-structure visible. The storage of RF-KET at a temperature close to its T_g drastically increases molecular mobility, thus facilitating recrystallization of the drug. Additionally, RF-KET contains 50% (w/w) Methocel, a very hydrophilic polymer, which can take up significant amounts of water thereby aiding in KET crystallization. In fact, visual evidence of moisture uptake was observed; the free-flowing RF-KET powder granules turned into sticky, non-free-flowing aggregated lumps, which were very difficult to handle.

In contrast, a significant delay in the onset of crystallization was observed for samples coated with a low and medium thickness CF_x-coating. A single endothermic peak corresponding to the melting of crystalline KET was observed after two and four months for RF-KET-CF_x low and medium, respectively. Also, melting endotherms were less pronounced for RF-KET-CF_x medium than for RF-KET-CF_x low, suggesting the CF_x medium coating provided enhanced protection against crystallization of KET. SEM pictures of RF-KET-CF_x low and medium (Fig. 7b and c) taken after 6 months of storage at elevated temperature and humidity show scattered regions with crystals at the surface. Compared to RF-KET-CF_x low and medium, RF-KET-CF_x high offered superior stability with no crystallization of KET observed even after 6 months of storage (longest time of observation).

Several studies have proposed the presence of a mobile surface layer in amorphous materials [14,46,47]. For example, Kajiyama and coworkers have reported that the molecular mobility on the surface of amorphous polystyrene films was notably increased compared to the bulk due to surface segregation of chain end groups [46]. It has been suggested that high surface mobility enables surface-initiated crystallization of amorphous compounds and therefore presents a general source of instability [14]. Studies have shown that gold and electrolyte coatings as thin as 10 nm were able to reduce molecular mobility and consequently prevent crystal growth at the surface of amorphous drugs [14,15].

The results of our stability study demonstrate that thin films polymerized by PPECVD using C_6F_{14} as the monomer were successfully able to reduce surface mobility as indicated by prevention of KET crystallization over a period of several months. Since the fluorocarbon coating chosen in this study is particularly hydrophobic, it not only presents a barrier against molecular mobility but also against moisture penetration. A previous study conducted by Vaswani et al. demonstrated that moisture uptake by different fluorocarbon films deposited on cellulose materials was less than 0.14 wt.% [30]. In contrast to uncoated RF-KET, all plasma-coated samples remained free-flowing during stability testing, indicating that no or little water uptake occurred.

Overall, it is evident that the effectiveness of the coating depends on its thickness or strictly speaking the surface coverage. XPS and ToF-SIMS results suggest that the RF-KET-CF_x low and medium surface coatings are not 100% covered with coating material. This means some areas of the RF-KET matrix were directly exposed to the surrounding environment allowing for increased surface mobility and moisture uptake, leading to localized crystal growth of KET.

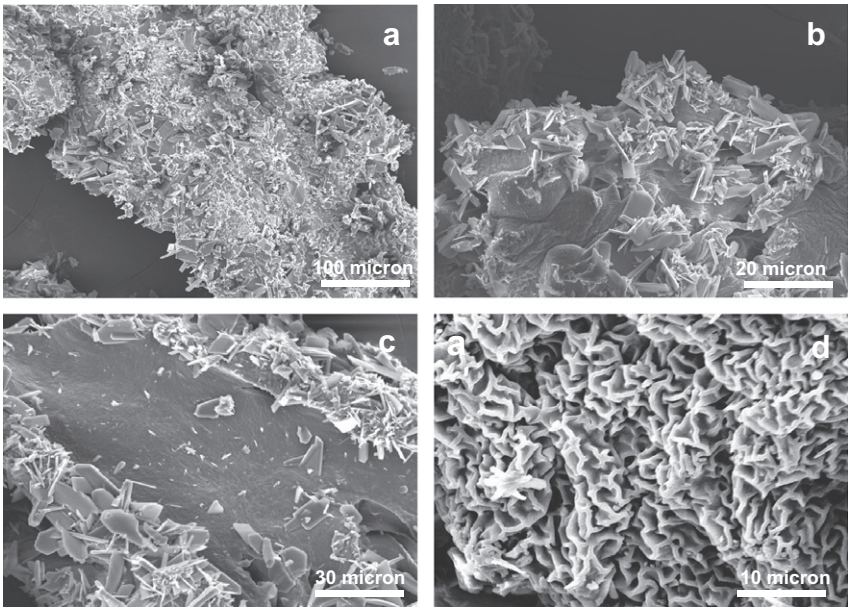

Fig. 7. SEM images of samples exposed to 40 °C and 75% RH (a) RF-KET (RF processed ketoprofen:Methocel™ E5 = 1:1) 2 weeks, (b) RF-KET-CF_x low 6 months, (c) RF-KET-CF_x medium 6 months, (d) RF-KET-CF_x high 6 months.

4. Conclusion

The influence of coating thickness of hydrophobic plasma-polymerized films on the crystallization of amorphous KET was investigated. All coated samples significantly decreased the onset of crystallization of the amorphous KET formulation, indicating the coating presented an effective barrier against surface mobility and moisture uptake. The extent of surface coverage, which increased with increasing coating thickness, was identified as the most important factor affecting the onset of crystallization. Higher surface coverage as achieved with RF-KET-CF_x high resulted in enhanced protection against crystallization for up to 6 months (longest time of observation) compared to only three days for uncoated material. In addition, a higher coating thickness is associated with decreased adhesion of the coating to the substrate, which was shown to be beneficial in the dissolution process. Overall, PPECVD represents a promising novel way to increase stability of amorphous drugs through surface modification.

Acknowledgment

The authors would like to thank ION-TOF for carrying out ToF-SIMS analysis on selected samples.

References

[1] L.R. Hilden, K.R. Morris, Physics of amorphous solids, J. Pharm. Sci. 93 (2004) 3–12.
[2] D. Singhal, W. Curatolo, Drug polymorphism and dosage form design: a practical perspective, Adv. Drug Deliv. Rev. 56 (2004) 335–347.
[3] L. Yu, Amorphous pharmaceutical solids: preparation, characterization and stabilization, Adv. Drug Deliv. Rev. 48 (2001) 27–42.
[4] S. Yoshioka, V.J. Stella, Stability of Drugs and Dosage Forms, Academic Kluwer, New York, NY, 2002.
[5] C. Ahlneck, G. Zografi, The molecular basis of moisture effects on the physical and chemical stability of drugs in the solid state, Int. J. Pharm. 62 (1990) 87–95.
[6] G. Zografi, States of water associated with solids, Drug Dev. Ind. Pharm. 14 (1988) 1905–1926.
[7] T. Vasconcelos, B. Sarmento, P. Costa, Solid dispersions as strategy to improve oral bioavailability of poor water soluble drugs, Drug Discov. Today 12 (2007) 1068–1075.
[8] R.J. Chokshi, N.H. Shah, H.K. Sandhu, A.W. Malick, H. Zia, Stabilization of low glass transition temperature indomethacin formulations: impact of polymer-type and its concentration, J. Pharm. Sci. 97 (2008) 2286–2298.
[9] H. Konno, T. Handa, D.E. Alonzo, L.S. Taylor, Effect of polymer type on the dissolution profile of amorphous solid dispersions containing felodipine, Eur. J. Pharm. Biopharm. 70 (2008) 493–499.
[10] D.Q.M. Craig, P.G. Royall, V.L. Kett, M.L. Hopton, The relevance of the amorphous state to pharmaceutical dosage forms: glassy drugs and freeze dried systems, Int. J. Pharm. 179 (1999) 179–207.
[11] L.S. Taylor, G. Zografi, Spectroscopic characterization of interactions between PVP and indomethacin in amorphous molecular dispersions, Pharm. Res. 14 (1997) 1691–1698.
[12] K. Khougaz, S.D. Clas, Crystallization inhibition in solid dispersions of MK-0591 and poly(vinylpyrrolidone) polymers, J. Pharm. Sci. 89 (2000) 1325–1334.
[13] H. Konno, L.S. Taylor, Ability of different polymers to inhibit the crystallization of amorphous felodipine in the presence of moisture, Pharm. Res. 25 (2008) 969–978.
[14] T. Wu, Y. Sun, N. Li, M.M. de Villiers, L. Yu, Inhibiting surface crystallization of amorphous indomethacin by nanocoating, Langmuir 23 (2007) 5148–5153.
[15] L. Zhu, L. Wong, L. Yu, Surface-enhanced crystallization of amorphous nifedipine, Mol. Pharm. 5 (2008) 921–926.
[16] S. Bose, R.H. Bogner, Solventless pharmaceutical coating processes: a review, Pharm. Dev. Technol. 12 (2007) 115–131.
[17] Y.F. Luo, J. Zhu, Y.L. Ma, H. Zhang, Dry coating, a novel coating technology for solid pharmaceutical dosage forms, Int. J. Pharm. 358 (2008) 16–22.
[18] H. Kage, R. Abe, R. Hattanda, T. Zhou, H. Ogura, Y. Matsuno, Effect of solid circulation rate on coating efficiency and agglomeration in circulating fluidized bed type coater, Powder Technol. 130 (2003) 203–210.
[19] J. Zhang, F. Zhu, C. Shi, L. Sun, Y. Wang, Z. Cheng, P.J.Q. Yang, Y. Guo, R. Zhou, H. Xie, W.J. van Ooij, J. Lian, D. Shi, Molecular tailoring coating on TiO_2 nanoparticle surface by plasma polymerization, in: R. d'Agostino, P. Favia, C. Oehr, M.R. Wertheimer (Eds.), Plasma Processes and Polymers, Wiley-VCH Verlag GmbH, Weinheim, Germany, 2005, pp. 117–128.
[20] C. Cavallotti, M. Di Stanislao, S. Carra, Interplay of physical and chemical aspects in the PECVD and etching of thin solid films, Prog. Cryst. Growth Charact. Mater. 48–49 (2004) 123–165.
[21] C.L. Rinsch, X.L. Chen, V. Panchalingam, R.C. Eberhart, J.H. Wang, R.B. Timmons, Pulsed radio frequency plasma polymerization of allyl alcohol: controlled deposition of surface hydroxyl groups, Langmuir 12 (1996) 2995–3002.
[22] R. Forch, A.N. Chifen, A. Bousquet, H.L. Khor, M. Jungblut, L.Q. Chu, Z. Zhang, I. Osey-Mensah, E.K. Sinner, W. Knoll, Recent and expected roles of plasma-polymerized films for biomedical applications, Chem. Vap. Depos. 13 (2007) 280–294.
[23] N. Gomathi, A. Sureshkumar, S. Neogi, RF plasma-treated polymers for biomedical applications, Curr. Sci. 94 (2008) 1478–1486.
[24] C. Susut, R.B. Timmons, Plasma enhanced chemical vapor depositions to encapsulate crystals in thin polymeric films: a new approach to controlling drug release rates, Int. J. Pharm. 288 (2005) 253–261.
[25] S.H. Su, R.Y.N. Chao, C.L. Landau, K.D. Nelson, R.B. Timmons, R.S. Meidell, R.C. Eberhart, Expandable bioresorbable endovascular stent. I. Fabrication and properties, Ann. Biomed. Eng. 31 (2003) 667–677.
[26] K.A. Overhoff, J.D. Engstrom, B. Chen, B.D. Scherzer, T.E. Milner, K.P. Johnston, R.O. Williams, Novel ultra-rapid freezing particle engineering process for enhancement of dissolution rates of poorly water-soluble drugs, Eur. J. Pharm. Biopharm. 65 (2007) 57–67.
[27] C.L. Chapman, D. Bhattacharyya, R.C. Eberhart, R.B. Timmons, C.J. Chuong, Plasma polymer thin film depositions to regulate gas permeability through nanoporous track etched membranes, J. Membr. Sci. 318 (2008) 137–144.
[28] M.P. Krafft, J.G. Riess, Perfluorocarbons: life sciences and biomedical uses – dedicated to the memory of Professor Guy Ourisson, a true RENAISSANCE man, J. Polym. Sci. Part A: Polym. Chem 45 (2007) 1185–1198.
[29] Z. Mana, Y. Pellequer, A. Lamprecht, Oil-in-oil microencapsulation technique with an external perfluorohexane phase, Int. J. Pharm. 338 (2007) 231–237.
[30] S. Vaswani, J. Koskinen, D.W. Hess, Surface modification of paper and cellulose by plasma-assisted deposition of fluorocarbon films, Surf. Coat. Technol. 195 (2005) 121–129.
[31] D. Bhattacharyya, K. Pillai, O.M.R. Chyan, L.P. Tang, R.B. Timmons, A new class of thin film hydrogels produced by plasma polymerization, Chem. Mater. 19 (2007) 2222–2228.
[32] C.M. Weikart, H.K. Yasuda, Modification, degradation, and stability of polymeric surfaces treated with reactive plasmas, J. Polym. Sci. Polym. Chem. 38 (2000) 3028–3042.
[33] P. Di Martino, E. Joiris, R. Gobetto, A. Masic, G.F. Palmieri, S. Martelli, Ketoprofen-poly(vinylpyrrolidone) physical interaction, J. Cryst. Growth 265 (2004) 302–308.
[34] M. Gordon, J.S. Taylor, Ideal copolymers and the second order transitions of synthetic rubbers I. Non-crystalline copolymers, J. Appl. Chem. 2 (1952) 493–500.
[35] R. Simha, R.F. Boyer, On a general relation involving the glass temperature and coefficients of expansion of polymers, J. Chem. Phys. 37 (1962) 1003–1007.
[36] R. Nair, N. Nyamweya, S. Gonen, L.J. Martinez-Miranda, S.W. Hoag, Influence of various drugs on the glass transition temperature of poly(vinylpyrrolidone): a thermodynamic and spectroscopic investigation, Int. J. Pharm. 225 (2001) 83–96.
[37] A.M. Hynes, M.J. Shenton, J.P.S. Badyal, Pulsed plasma polymerization of perfluorocyclohexane, Macromolecules 29 (1996) 4220–4225.
[38] N.M. Mackie, N.F. Dalleska, D.G. Castner, E.R. Fisher, Comparison of pulsed and coupled continuous-wave deposition of thin films from saturated fluorocarbon/H-2 inductively rf plasmas, Chem. Mater. 9 (1997) 349–362.
[39] Y.L. Wu, L.C.M. Han, B.E. Thomes, H.B. Qiu, C.R. Savage, W.W. Lee, R.B. Timmons, Pulsed plasma polymerizations: film chemistry control and applications, in: W.W. Lee, R. Dagostino, M.R. Wertheimer (Eds.), Plasma Deposition and Treatment of Polymers, Materials Research Society, Warrendale, 1999, pp. 77–87.
[40] E.J. Winder, K.K. Gleason, Growth and characterization of fluorocarbon thin films grown from trifluoromethane (CHF3) using pulsed-plasma enhanced CVD, J. Appl. Polym. Sci. 78 (2000) 842–849.
[41] S.M. Mukhopadhyay, P. Joshi, S. Datta, J.G. Zhao, P. France, Plasma assisted hydrophobic coatings on porous materials: influence of plasma parameters, J. Phys. D: Appl. Phys. 35 (2002) 1927–1933.
[42] A.S.D. Sobrinho, G. Czeremuszkin, M. Latreche, M.R. Wertheimer, Defect-permeation correlation for ultrathin transparent barrier coatings on polymers, J. Vac. Sci. Technol. A 18 (2000) 149–157.
[43] M. Hanika, H.C. Langowski, U. Moosheimer, W. Peukert, Inorganic layers on polymeric films – influence of defects and morphology on barrier properties, Chem. Eng. Technol. 26 (2003) 605–614.
[44] G. GarciaAyuso, L. Vazquez, J.M. MartinezDuart, Atomic force microscopy (AFM) morphological surface characterization of transparent gas barrier coatings on plastic films, Surf. Coat. Technol. 80 (1996) 203–206.
[45] F. Lewis, P. Horny, P. Hale, S. Turgeon, M. Tatoulian, D. Mantovani, Study of the adhesion of thin plasma fluorocarbon coatings resisting plastic deformation for stent applications, J. Phys. D: Appl. Phys. 41 (2008) 7.
[46] T. Kajiyama, K. Tanaka, A. Takahara, Study of the surface glass transition behaviour of amorphous polymer film by scanning-force microscopy and surface spectroscopy, Polymer 39 (1998) 4665–4673.
[47] S. Kawana, R.A.L. Jones, Character of the glass transition in thin supported polymer films, Phys. Rev. E 63 (2001) 6.